Clinical Cancer Research

miRNA Landscape in Stage I Epithelial Ovarian Cancer Defines the Histotype Specificities

Enrica Calura, Robert Fruscio, Lara Paracchini, et al.

Updated version	Access the most recent version of this article at: doi:10.1158/1078-0432.CCR-13-0360
Supplementary Material	Access the most recent supplemental material at: http://clincancerres.aacrjournals.org/content/suppl/2013/06/13/1078-0432.CCR-13-0360.DC1.html

Cited Articles	This article cites by 37 articles, 17 of which you can access for free at: http://clincancerres.aacrjournals.org/content/19/15/4114.full.html#ref-list-1

E-mail alerts	Sign up to receive free email-alerts related to this article or journal.
Reprints and Subscriptions	To order reprints of this article or to subscribe to the journal, contact the AACR Publications Department at pubs@aacr.org.
Permissions	To request permission to re-use all or part of this article, contact the AACR Publications Department at permissions@aacr.org.

miRNA Landscape in Stage I Epithelial Ovarian Cancer Defines the Histotype Specificities

Enrica Calura[1], Robert Fruscio[2,4], Lara Paracchini[5], Eliana Bignotti[6], Antonella Ravaggi[6], Paolo Martini[1], Gabriele Sales[1], Luca Beltrame[5], Luca Clivio[5], Lorenzo Ceppi[2,4], Mariacristina Di Marino[5], Ilaria Fuso Nerini[5], Laura Zanotti[6], Duccio Cavalieri[8], Giorgio Cattoretti[3], Patrizia Perego[3], Rodolfo Milani[2,4], Dionyssios Katsaros[9,4], Germana Tognon[7,4], Enrico Sartori[7], Sergio Pecorelli[6,7], Costantino Mangioni[2,4], Maurizio D'Incalci[4,5], Chiara Romualdi[1], and Sergio Marchini[5]

Abstract

Purpose: Epithelial ovarian cancer (EOC) is one of the most lethal gynecologic diseases, with survival rate virtually unchanged for the past 30 years. EOC comprises different histotypes with molecular and clinical heterogeneity, but up till now the present gold standard platinum-based treatment has been conducted without any patient stratification. The aim of the present study is to generate microRNA (miRNA) profiles characteristic of each stage I EOC histotype, to identify subtype-specific biomarkers to improve our understanding underlying the tumor mechanisms.

Experimental Design: A collection of 257 snap-frozen stage I EOC tumor biopsies was gathered together from three tumor tissue collections and stratified into independent training ($n = 183$) and validation sets ($n = 74$). Microarray and quantitative real-time PCR (qRT-PCR) were used to generate and validate the histotype-specific markers. A novel dedicated resampling inferential strategy was developed and applied to identify the highest reproducible results. mRNA and miRNA profiles were integrated to identify novel regulatory circuits.

Results: Robust miRNA markers for clear cell and mucinous histotypes were found. Specifically, the clear cell histotype is characterized by a five-fold (log scale) higher expression of *miR-30a* and *miR-30a**, whereas mucinous histotype has five-fold (log scale) higher levels of *miR-192/194*. Furthermore, a mucinous-specific regulatory loop involving *miR-192/194* cluster and a differential regulation of *E2F3* in clear cell histotype were identified.

Conclusions: Our findings showed that stage I EOC histotypes have their own characteristic miRNA expression and specific regulatory circuits. *Clin Cancer Res; 19(15); 4114–23. ©2013 AACR.*

Introduction

Despite the increasing molecular knowledge of tumor biology which underpins the development of new thera-peutic and clinical management strategies, epithelial ovarian cancer (EOC) is one of the most lethal gynecologic diseases, with a 5-years survival rate virtually unchanged for the past 30 years (1).

Notwithstanding the enormous effort, the causes of its pathogenesis are still unknown as well as the mechanism of disease in the early phases of the carcinogenesis. Most EOC studies have been conducted in patients characterized by stage III/IV, the most frequent clinical manifestation, whereas the low incidence of stage I EOCs has hampered the possibility to collect sizable cohorts of tumor biopsies and to conduct stage I dedicated studies.

The importance of a better knowledge of stage I EOC is particularly made evident by the recent proposal about the EOC origin described by Kurman and Shih (1). On the basis of this theory, all histologic types, of what we currently define "ovarian carcinoma," originate from different organs sharing the same anatomic location.

Low-grade serous, mucinous, endometrioid, and clear cell histotypes represent the great majority of type I EOCs, which usually have a slow progression rate, are generally confined to the ovary, lack of p53 mutations,

Authors' Affiliations: [1]Department of Biology, University of Padova, Via U. Bassi, Padova; [2]Clinic of Obstetrics and Gynecology; [3]Department of Pathology, University of Milano-Bicocca, San Gerardo Hospital, Via Per-golesi, Monza; [4]IRCCS - "Mario Negri" Gynecological Oncology group (MaNGO); [5]Department of Oncology, IRCCS - Istituto di Ricerche Farm-acologiche "Mario Negri", via La Masa, Milano; [6]Division of Gynecologic Oncology, "Angelo Nocivelli" Institute of Molecular Medicine; [7]Department of Obstetrics and Gynecology, University of Brescia, Viale Europa, Brescia; [8]Research and Innovation Center, Fondazione Edmund Mach, Via E. Mach, San Michele all'Adige, Trento; and [9]Department of Gynecology/Oncology, S. Anna Hospital, University of Torino, Corso Spezia, Torino, Italy

American Association for Cancer Research

Translational Relevance

The present study shows that different histotypes of stage I ovarian cancer exhibit divergent microRNA (miRNA) profiles, thus supporting the hypothesis that ovarian tumors with different histotypes are biologically distinct and thus they should be treated as different neoplastic diseases.

In particular, the pattern of expression of some miRNAs was found specific for clear cell or for mucinous ovarian carcinomas, a finding of potential diagnostic and therapeutic importance.

and show a lineage with the corresponding benign neoplasm through an intermediate step called borderline tumor stage (1). This notion is not universally accepted; however, there is a general consensus on the heterogeneous molecular and clinical characteristics of the different EOC histotypes (2).

Köbel and colleagues, in a retrospective study, tested 21 candidate markers in a cohort of 500 advanced stages EOCs, showing that the association between biomarker expressions and survival rates varies among subtypes. The results suggest that the different histologic types are indeed distinct diseases, intimating that including different histotypes in a single cohort may not only confound survival analyses, but also it can lead to erroneous conclusions (3).

The role of microRNAs (miRNA) in high-grade EOCs has been studied in the past, highlighting a strong involvement of both the noncoding RNAs and the enzymes composing the miRNA-processing machinery (4, 5). Data previously published by our group deciphered a molecular circuit in stage I EOC, revealing miR-200c as an independent prognostic factor (6, 7). Focusing our study on the miRNA profiles, we studied the differences among stage I EOC histologic types looking for specific markers and regulatory circuits. The histotype specificities are key knowledge to understand the treatment efficacies and to guide the development of new therapies. At the same time, a better characterization of early EOCs can be potentially helpful to deeply clarify the mechanism of the disease.

Here, we present the first retrospective study focused on histotypes, exclusively based on stage I EOC samples, including a collection of 257 snap-frozen tumor biopsies gathered by 3 independent tumor tissue banks.

Materials and Methods

Tissue sample collection

A cohort of 257 snap-frozen tumor biopsies was gathered together from 3 independent snap-frozen tumor tissue collections (Supplementary Section S1). Tumor tissue samples, collected at the time of surgery, were sharp dissected and snap frozen in liquid nitrogen within 15 minutes from resection, and then stored at $-80°C$. Patients underwent a complete staging procedure, according to the International Federation of Gynecological and Obstetrics criteria (8). All biopsies selected for the study belonged to patients naïve to chemotherapy and with diagnosis of stage I EOC.

All patients with a suspected mucinous ovarian cancer underwent preoperative colonoscopy and gastroscopy, to exclude metastatic disease from a gastrointestinal tumor. Even when the diagnosis of mucinous histology was made postoperatively, patients underwent endoscopic examinations within 1 month from surgery. Patients who were found to have ovarian metastases from gastrointestinal tumors were not considered for the present study.

Clinical and anatomopathologic patient information was registered, and follow-up data were obtained from periodic gynecologic and oncological check-up. Clinical data were analyzed following the procedures described in Supplementary Section S2. The tumor content of the specimens was assessed by hematoxylin and eosin staining to check epithelial purity. Although malignant cells content in borderline tumors ranged from 45% to 70%, in malignant tumors only specimens containing more than 70% of the epithelial tumor cells were used. Tumor grade and histologic type were determined following World Health Organization standards. A written informed consent was obtained from all the patients enrolled in the study, which has been conducted following the Declaration of Helsinki set of principles. The local scientific ethical committees of all the centers participating to the study approved the collection and the use of tumor samples. Human Ovarian Surface Epithelium (HOSE) primary cell lines were established after sterile processing of samples from surgical biopsies, as described in Supplementary Section S3.

Expression experiments and analyses

miRNA extraction, labeling, and hybridization were conducted as previously published (7) and more details are described in Supplementary Section S4. miRNA profiles raw data have been submitted to ArrayExpress (E-MTAB-1067). A resampling strategy methodology was applied as described in Supplementary Section S5. Gene expression dataset (B1 collection; GSE8841-2; ref. 6) was treated following the Supplementary Section S6 procedure, and MAGIA2 software (9, 10) was used to conduct the integrative analysis.

Validation using qRT-PCR

miRNA and gene expression levels were validated by quantitative real-time PCR (qRT-PCR) using Sybr Green protocol (Qiagen) on an Applied Biosystems 7900HT instrument. Experiments were run in triplicate, using 384-well reaction plates in an automatic liquid handling station (epMotion 5075LH; Eppendorf). Analysis was conducted as previously described (7), using 4 independent housekeeping genes as listed in Supplementary Section S7. Two-sided Student t test for training set and Wilcoxon test for validation set were used to verify among groups mean differences. P values < 0.05 were considered statistically significant.

Luciferase assays

pmirGLO-*CUL4* (pCUL4), pmirGLO-*PSME3* (pPSME3), and psiCHECK-*BMI1* (pBMI1) plasmids, containing predicted miRNA-binding sites for *miR-194*, were PCR subcloned into the pmirGLO or psiCHECK-2 luciferase reporter plasmid using primers pair sequences reported in Supplementary Section S7, as follows: 95°C for 1 minute (1 cycle); 95°C for 30 seconds, annealing temperature for 1 minute, 68°C for 2 minutes (40 cycles), and a final extension step at 68°C for 1 minute (see Supplementary Table S7.1 for different annealing temperature). Human embryonic kidney (HEK) 293 cells, originally obtained from American Type Culture Collection, routinely grown at 37°C, 5% CO_2 in Dulbecco's modified Eagle medium (Life Technologies), supplemented with 10% FBS (Lonza) and 1% L-glutamine 200 mmol/L (Biowest) were used for luciferase assay. HEK 293 cells were tested and authenticated by short tandem repeat profile using the Cell ID System (Promega) and ABI Prism 310 Genetic Analyzer (Applied Biosystems), before last freezing (November 2012).

Subconfluent HEK 293 cells, seeded in 96-well reaction plates, were cotransfected with plasmids (10 ng) and with 2 pmol of synthesized, double-stranded *miRNA-194* (or siRNA scramble; Qiagen) using Lipofectamine 2000 (Life Technologies). Twenty-four hours after transfection, firefly and *Renilla* luciferase activity was measured consecutively in a microplate reader (Tecan Infinite M200) using the Dual Luciferase Assay System (Promega). Cotransfection of psiCHECK-*ZEB1* (pZEB1, kindly provided by Dr. Goodall, Centre for Cancer Biology SA Pathology Frome Road, Adelaide SA 5000, Australia) with synthetic *miR-200c* (Qiagen) was used as positive control. Empty vectors were transfected as negative controls. Each sample was assayed in 6 replicates and repeated twice.

Results

Patient characteristics

To identify a miRNA signature able to characterize EOC histotypes, we analyzed a collection of 257 snap-frozen tumor biopsies obtained from primary surgery on stage I EOC patients naïve to chemotherapy, gathered together from 3 tumor tissue collections hereafter called A, B, and C (Supplementary Section S1).

Given that borderline ovarian tumors are histologically characterized as epithelial tumors, they are included in the study, even if they are defined as low malignant potential tumors. Borderline patients, mainly with serous and mucinous histology, represented the approximately 20% of the entire patient cohort (38 patients in the training set, 15 patients in the validation set). Aware of the fact that the borderline inclusion criteria could be considered controversial, all the analyses reported in this study were conducted including and excluding borderline patients, with overlapping results.

Median patient ages at diagnosis in the 3 collections were similar, as well as the distribution among histotypes and grades of nuclear differentiation.

As previously reported in different early-stage EOC-dedicated studies (11–13), both univariate and multivariate analyses did not reveal any difference in survival rates among different histotypes. The grade of tumor was the most significant prognostic feature: increasing grade at the time of diagnosis was associated to decrease in patient survival (Supplementary Section S2). This result confirmed that our cohort of patients is consistent with data reported in the literature for stage I EOC and that is both representative of clinical settings and suitable for downstream analyses.

A schematic representation of the experimental and computational strategies adopted in this study is reported in the flow chart of Fig. 1. The entire cohort of patients was subdivided into a training set ($n = 183$; collection A, B1, and B2) and a validation set ($n = 74$; collection B3 and C). The training set was used to: (i) generate miRNA expression profiles and define marker identification procedure (A+B1+B2), (ii) integrate miRNA profiles with gene expression patterns (6) in a subset of patients (B1), and (iii) validate gene and miRNA expression by qRT-PCR (A+B1+B2). The validation set was used only to independently validate the expression by qRT-PCR.

Analysis of microRNA landscape

To measure the miRNA expression in a high-throughput manner, training set biopsies ($n = 183$) were profiled using microarray. Figure 2A shows the heatmap of the 250 miRNA values obtained after the preprocessing and data normalization. On a global scale, a large part of the entire set of miRNAs was similar across samples, and it does not help to separate patients by histotype and grade. Then, the expression levels have been analyzed and Supplementary Section S4 shows the lists of significantly deregulated miRNAs for each subtype comparison, including and excluding borderline samples. It is noteworthy that, among all the different comparisons, the mucinous subtype showed the highest number of differentially expressed features when compared with the other subtypes (Fig. 2B). If the number of differentially expressed miRNAs is a measure of the differences among histologic types, our results support the hypothesis that the mucinous subtype is markedly different from all the others.

Although all the miRNAs reported above have significant adjusted *P* value due to patient variability among subtypes, only few of them can be exploited as subtype-specific markers, which are miRNAs that almost perfectly predict the histotype of independent samples. Then, with the aim to identify miRNA markers among those differentially expressed, we conducted a dedicated resampling strategy (Supplementary Section S5). A resampling score was assigned to each miRNA, following the rule that the higher the score, the higher is the prediction power. Only 10 miRNAs were found commonly deregulated across all possible comparisons of subtypes, and only 3 miRNAs reached the maximum score: *miR-192* and *miR-194* were highly expressed in the mucinous subtype, and *miR-30a* was highly expressed in clear cell EOCs. Otherwise, no miRNA could be identified as potential marker for endometrioid or serous histotypes. Thus, we reasoned that

Figure 1. Flow chart of the experimental and computational strategies of the study.
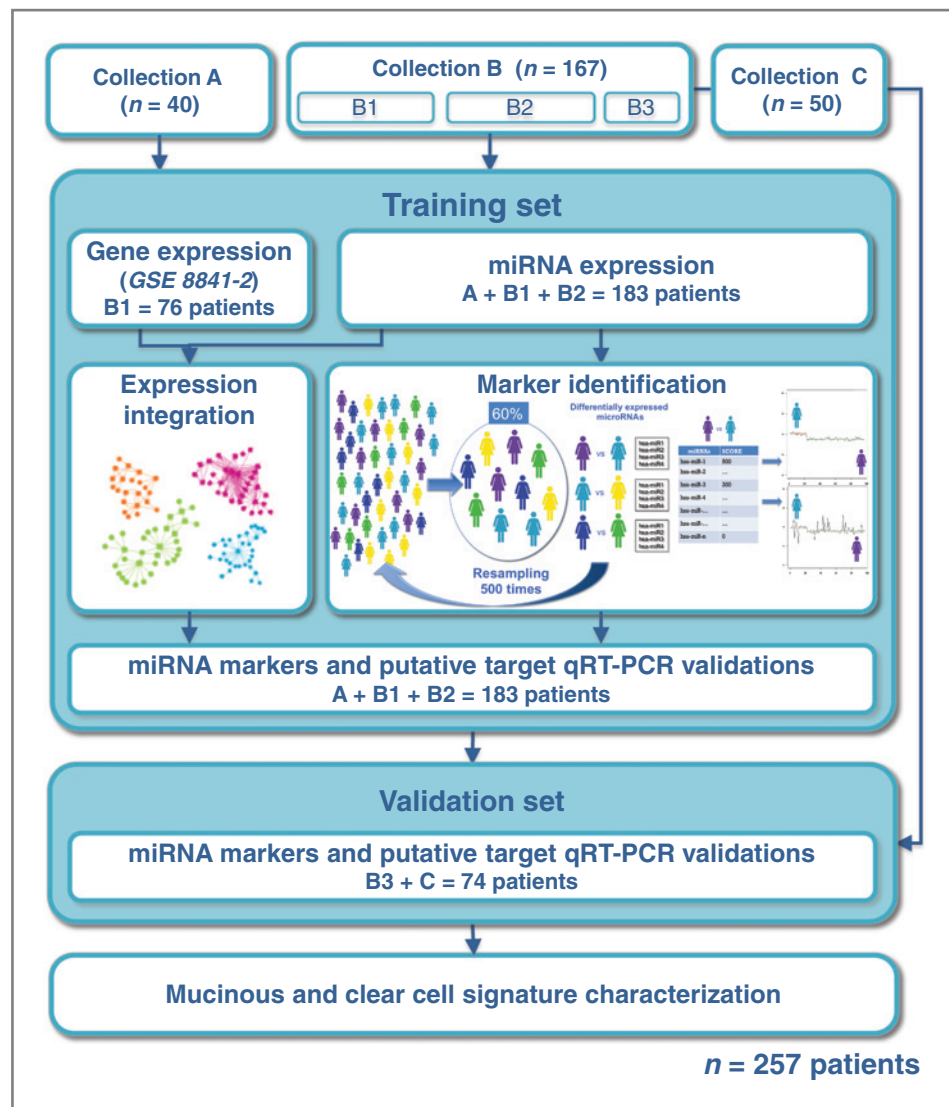
miR-192/194 and miR-30a could be considered EOC histotype-specific markers. Although characterized by a high resampling score, miR-30a* did not reach the resampling score maximum in all comparisons. However, due to its physical association with miR-30a, it was included in the list of miRNAs selected for validations. It is to note that, repeating the analyses excluding the borderline samples, the results obtained were similar (Table 1 and Supplementary Section S4). In Fig. 2C, we reported the distribution of miRNA expression levels of miR-192/194 and miR-30a/30a* in the 4 histotypes. Using these expression profiles to recluster the entire set of patients, we obtained the cluster in Fig. 2D. The classification of subtypes improved dramatically, separating mucinous and clear cell histotypes from the others, whereas endometrioid and serous sample subtypes, as expected, generated a single and heterogeneous cluster. Interestingly, the mucinous cluster in Fig. 2D was preferentially characterized by the presence of low-grade patients (grade 1

and borderline). Given this evidence, we investigated the presence of potential variability in expression level across grades within subtypes. We found that, although not significant, miR-192/194 expression levels slowly decreased with the increasing grade and, interestingly, this decrease was associated with reduced survival (Supplementary Section S8). Taken together, our results show that, independent of inclusion criteria (i.e., considering or excluding borderline tumors), miR-192/194 and miR-30a/30a* are histotype-specific markers for stage I EOC.

Moreover, to assess whether miR-192/194 and miR-30a/30a* were tumor-specific markers, we compared the miRNA expression of EOC histotypes with those of HOSE cells, derived from normal ovarian epithelial tissue of patients undergoing surgery for benign pathologies (Supplementary Materials S3). We conducted expression measurements using both microarray and qRT-PCR.

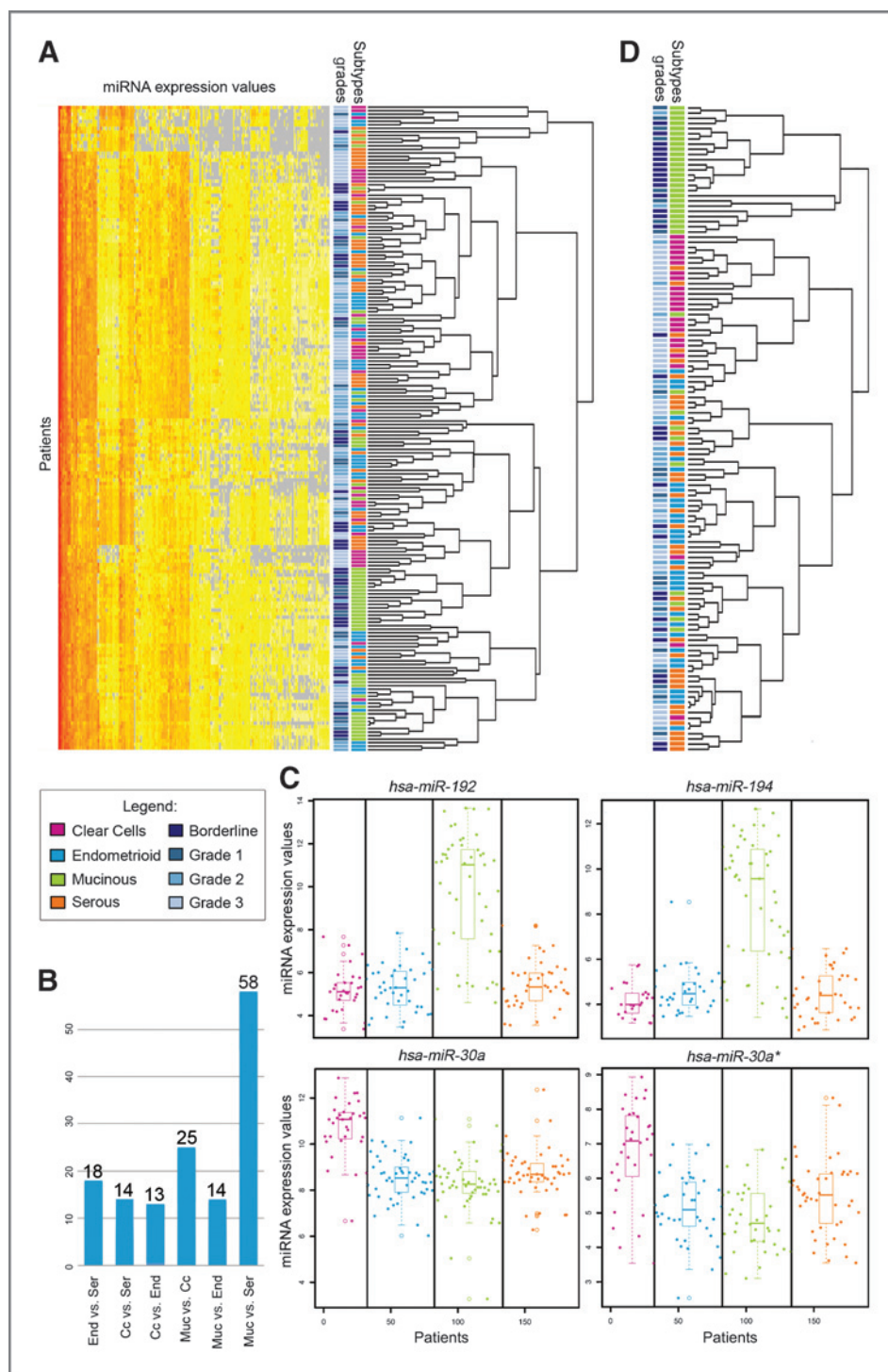Data reported in Supplementary Fig. S3.1 show that the number of miRNAs, found differentially expressed between

Figure 2. Microarray data analyses. A, heatmap with cluster analysis on miRNA and samples using all the expression profiles. B, barplots showing the number of differentially expressed miRNAs across subtype comparisons. C, scatterplots and boxplots of the 4 miRNA markers' expression values (*miR-194, miR-192, miR-30a*, and *miR-30a**) in patients divided by histotype. D, cluster analysis obtained using only the 4 subtype-specific miRNAs. Grade and subtypes are reported in different colors. Muc, mucinous; Cc, clear cell; Ser, serous; End, endometrioid.

HOSE and the EOC histotypes, was higher than the number reported for the comparison within the tumor histotypes. *miR-192/194* and *miR30a/30a** data, obtained using array (Supplementary Table S3.1) and qRT-PCR validations (Supplementary Table S3.2), indicated that the previously reported markers were not expressed in HOSE cells.

Relationship between miRNA and gene expression

To depict more in detail the molecular circuits behind each histotype, we focused on functional miRNA target relationships by approaching an *in silico* integration between miRNAs and gene expression profiles. A portion (B1, $n = 76$) of the patient cohort was previously used for gene expression analysis (GSE8841-2), and their clinical

Table 1. Microarray measurements of miRNA markers across histotypes

	miRNAs	Class comparison	With borderlines			Without borderlines		
			$\log_2(FC)$	adj. P	RS	$\log_2(FC)$	adj. P	RS
Mucinous	miR-192	Muc vs. Cc	4.58	2.36E-19	500	4.09	1.40E-13	500
		Muc vs. End	4.46	1.80E-21	500	4.01	2.03E-14	500
		Muc vs. Ser	4.29	1.93E-20	500	3.6	3.81E-11	500
	miR-194	Muc vs. Cc	4.49	1.27E-16	500	3.83	1.96E-11	500
		Muc vs. End	4.01	6.09E-17	500	3.39	1.65E-10	500
		Muc vs. Ser	4.15	2.75E-18	500	3.39	9.37E-10	500
Clear cell	miR-30a	Cc vs. End	2.18	6.94E-13	500	2.15	2.67E-11	500
		Cc vs. Muc	2.47	1.27E-16	500	2.63	5.37E-13	500
		Cc vs. Ser	1.99	8.08E-11	500	2.08	1.50E-09	500
	miR-30a*	Cc vs. End	1.62	4.67E-07	494	1.62	6.96E-06	475
		Cc vs. Muc	1.91	8.94E-10	500	2.00	3.14E-06	487
		Cc vs. Ser	1.28	8.72E-05	408	1.39	0.000424	316

NOTE: For each comparison, data including and excluding borderline tumors are shown.

Abbreviations: Muc, mucinous; Cc, clear cell; Ser, serous; End, endometrioid; $\log_2(FC)$, fold change is in $\log_2$ scale; adj. P, P values were adjusted for multiple testing; RS, resampling score.

features are reported in Supplementary Section S6 (6). Anticorrelated expressions were searched between miRNA and their putative target genes. We found miR-192/194 and miR-30a among the top results, confirming the prominent role of these miRNAs (Supplementary Section S6). Then, for downstream analyses, we chose the top significant and interesting anticorrelated targets of the 4 miRNA markers: BMI1, CIAO1, PSME3, CUL4A, MAPK4A, UBEV2V2, APOL1A, PTGER3, E2F3, ZNF64 (Supplementary Table S6.2).

Genes and miRNA validation

We measured by qRT-PCR the expression levels of miRNA markers and their selected putative targets in the training set and in an independent validation set (Fig. 1). To avoid potential errors due to batch effects, new batches of snap-frozen material for the entire cohort of samples were used. All the analyses were conducted including and excluding borderline patients, leading to the same results (Table 2 and Supplementary Section S7).

Within the training set, data show that miR-192/194 were, roughly in log scale, 5- to 8-fold overexpressed in mucinous compared with the other histotypes and miR-30a/30a* mirror the same trend, being in log scale 5- to 7-fold overexpressed in the clear cell compared with the other histotypes ($P < 0.001$). Seven out of the selected 10 putative target genes were confirmed by qRT-PCR (Supplementary Section S7).

In the validation set, miRNA markers ($P < 0.005$) and 6 of the 7 putative target genes ($P < 0.05$) previously confirmed in the training set, were reconfirmed. In particular, BMI1, CIAO1, PSME3, CUL4A, and PTGER3 were 3- to 4-fold (log scale) downregulated in the mucinous compared with the other subtypes, and E2F3 was approximately 4-fold (log scale) downregulated in the clear cell compared with the

other histotypes. For reason of completeness, also MDM2 and CDKN2A were included in the list of analyzed genes, because they belong to the same circuit. Boxplots in Fig. 3A summarize the qRT-PCR expression values of all the genes in the circuit, analyzed in all 257 patients enrolled in the study. BMI1, PSME3, CUL4A, and miR-192/194 showed expression concordant to the previous analyses, MDM2 was 3- to 4-fold in log scale downregulated, and CDKN2A was 3- to 5-fold in log scale upregulated in the mucinous histotype (Supplementary Table S7.6).

Functional binding assays: downstream target analysis

Among the genes of the circuit previously validated, not only BMI1, a known target of miR-194 (14), but also CUL4A and PMSE3 could be novel and attractive candidate targets. Luciferase reporter vectors containing the entire CUL4A, PSME3, and BMI1 3′UTR, with highly conserved miR-194-binding motif, were constructed and luciferase activity was assayed. Results, reported in Supplementary Fig. S7.4, showed that cotransfection of miR-194 with PSME3 or CUL4A 3′UTR did not inhibit luciferase activity, meaning that despite the anticorrelated expressions and the presence of a predicted binding site, miR-194 did not directly mediate the inhibition of PSME3 and CUL4A gene expression. On the other hand, when cotransfected with BMI1 3′UTR, miR-194 inhibited luciferase activity by approximately 30% and the difference is significant to the t test, confirming the results previously reported by Dong and colleagues (ref. 14; Supplementary Fig. S7.4).

Discussion

Since the introduction of platinum compounds in the EOC adjuvant treatment in the 1980s, there has been little improvement in the outcome. One of the possible explanations of the failure of virtually all clinical trials with new

Table 2. qRT-PCR measurements of miRNA markers across histotypes

	miRNAs	Class comparison	With borderlines				Without borderlines			
			Training set		Validation set		Training set		Validation set	
			$\log_2$(FC)	P	$\log_2$(FC)	P	$\log_2$(FC)	P	$\log_2$(FC)	P
Mucinous	miR-192	Muc vs. Cc	8.79	1.02E-22	11.46	5.36E-05	8.50	2.42E-15	10.63	1.24E-05
		Muc vs. End	6.90	6.22E-17	7.52	2.54E-07	6.77	7.03E-11	6.51	0.000157
		Muc vs. Ser	8.69	1.02E-28	6.98	8.59E-08	8.53	8.82E-17	6.61	0.000259
	miR-194	Muc vs. Cc	6.05	3.63E-11	7.30	0.0003	5.80	5.62E-08	6.16	0.001873
		Muc vs. End	5.31	1.32E-11	6.16	2.42E-06	5.22	2.93E-08	4.90	0.001240
		Muc vs. Ser	6.62	7.18E-17	5.73	7.33E-06	7.01	4.90E-13	4.63	0.001787
Clear cell	miR-30a	Cc vs. End	5.21	7.47E-20	6.43	1.80E-06	5.24	1.67E-19	6.31	9.24E-07
		Cc vs. Muc	5.40	1.88E-20	5.12	0.0045	5.38	1.99E-15	7.45	1.60E-05
		Cc vs. Ser	5.73	3.81E-22	5.25	5.16E-05	5.88	3.24E-19	5.84	1.78E-05
	miR-30a*	Cc vs. End	5.38	3.44E-09	7.12	1.80E-06	5.51	2.48E-09	6.99	2.75E-06
		Cc vs. Muc	6.10	1.37E-11	6.54	2.68E-05	6.48	6.36E-10	8.17	1.11E-06
		Cc vs. Ser	7.19	1.96E-15	6.63	2.72E-06	7.72	1.94E-15	7.05	2.21E-06

NOTE: For each comparison, data including and excluding borderline tumors are shown.
Abbreviations: Muc, mucinous; Cc, clear cell; Ser, serous; End, endometrioid; $\log_2$(FC), fold change is in $\log_2$ scale.

drugs in the last decades is that, most of them, as well as most of the EOC studies, did not consider any histotype patients stratifications. Focusing on miRNAs, that are highly tissue specific and have recently been identified as targets for therapeutic interventions, we investigated the expression and the role of miRNAs in the 4 EOC histotypes. The results of the analysis indicate an unambiguous miRNA marker set for clear cell (high levels of miR-30a/30a*) and mucinous subtypes (high levels of miR-192/194).

Clear cell subtype markers: miR-30a and miR-30a*

miR-30a/30a* are in log scale 5-fold more highly expressed in clear cell subtype than in the other subtypes, as well as in HOSE cells; unfortunately miR-30a* has hitherto not been well characterized. miR-30a negatively regulates BECLIN1, a positive regulator of the autophagy pathway (15), which is a tightly regulated catabolic process considered a key pathway in cancer, even if its role in carcinogenesis has not been fully elucidated (16). Nevertheless, these findings hint tantalizingly at a possible role of autophagy in determining the sensitivity and resistance to clear cell EOC therapy. At time of writing, the potential consequences of these data are not clear.

We found that miR-30a is significantly negatively correlated with E2F3 expression. Specifically, clear cell subtype has significantly lower levels of E2F3 compared with the other subtypes. E2F3 is a transcription factor crucially involved in EOC cell proliferation. It is a prognostic factor positively correlated with the grade of the disease (17, 18). Considering all the EOC stages together, Reimer and colleagues showed that (i) E2F3 levels are highly expressed in EOC compared with normal tissues, (ii) its expression increases with the increase in grade of the disease, and (iii)

all the histologic subtypes contribute equally to this increment of E2F3 expression. Unfortunately, their sample batch lacked clear cell subtype. In our clear cell samples, we registered a lower E2F3 expression compared with the other histotypes. Our results suggest that E2F3 underpins a different mechanism and regulation in the clear cell histotype compared with others, perhaps related to miR-30a differential expression. In studies of advanced stages EOC, miR-30a has been already found overexpressed in clear cell histotype (19, 20), thus indicating the possibility that miR-30a could be a stage-independent clear cell marker.

Mucinous subtype markers: miR-192 and miR-194

miR-192/194 were found to be much more expressed in mucinous than in the other subtypes and in HOSE cells. Borderline mucinous tumors, which are considered putative precursor lesions of malignant mucinous EOCs (2), have approximately the same expression level of miR-192/194 as the malignant mucinous counterpart.

miR-192/194 expression in mucinous samples shows only a slight decrease from borderline to grade 3 (Supplementary Section S8). According to our findings, low levels of miR-192/194 are known to be associated with a more malignant status in a panel of solid tumors (21–25), especially in colon and gastric tissues in which they are considered biomarkers (22, 24). The molecular similarity between mucinous EOC and the colon and gastric carcinomas invites to speculate that mucinous EOC should not be considered and of consequence treated, with the same regimes used for the other EOC histotypes. The integration of gene and miRNA expressions revealed a series of interesting putative targets of miR-192/194, among them were CIAO1, PTGER3, BMI1, PSME3, and CUL4A. CIAO1 is a member of the WD40 family of proteins, involved in iron–sulphur protein

Figure 3. Differential regulation of pathway upstream p53 in the EOC histotypes. A, genes and miRNAs qRT-PCR expression values of the circuit in the entire cohort of patients ($n = 257$). B, schema of the p53 circuit. Red and green in color bar represent high expression and low expression, respectively, in endometrioid (E), clear cell (C), mucinous (M), and serous (S) histotypes. BMI1 is a repressor of *CDKN2A* protein (32) that prevents the degradation and inactivation of p53 operated by *MDM2* (33). PSME3 and CUL4A, interacting with MDM2, promote the *TP53* degradation (30, 31). Moreover, TP53 is the transcription factor that controls the expression of *miR-192/194* cluster (27). Among the targets of this miRNA cluster, miR-194 downregulates *BMI1* and both *miR-192/194* target *MDM2* (14, 27). ***, $P < 1E-07$.
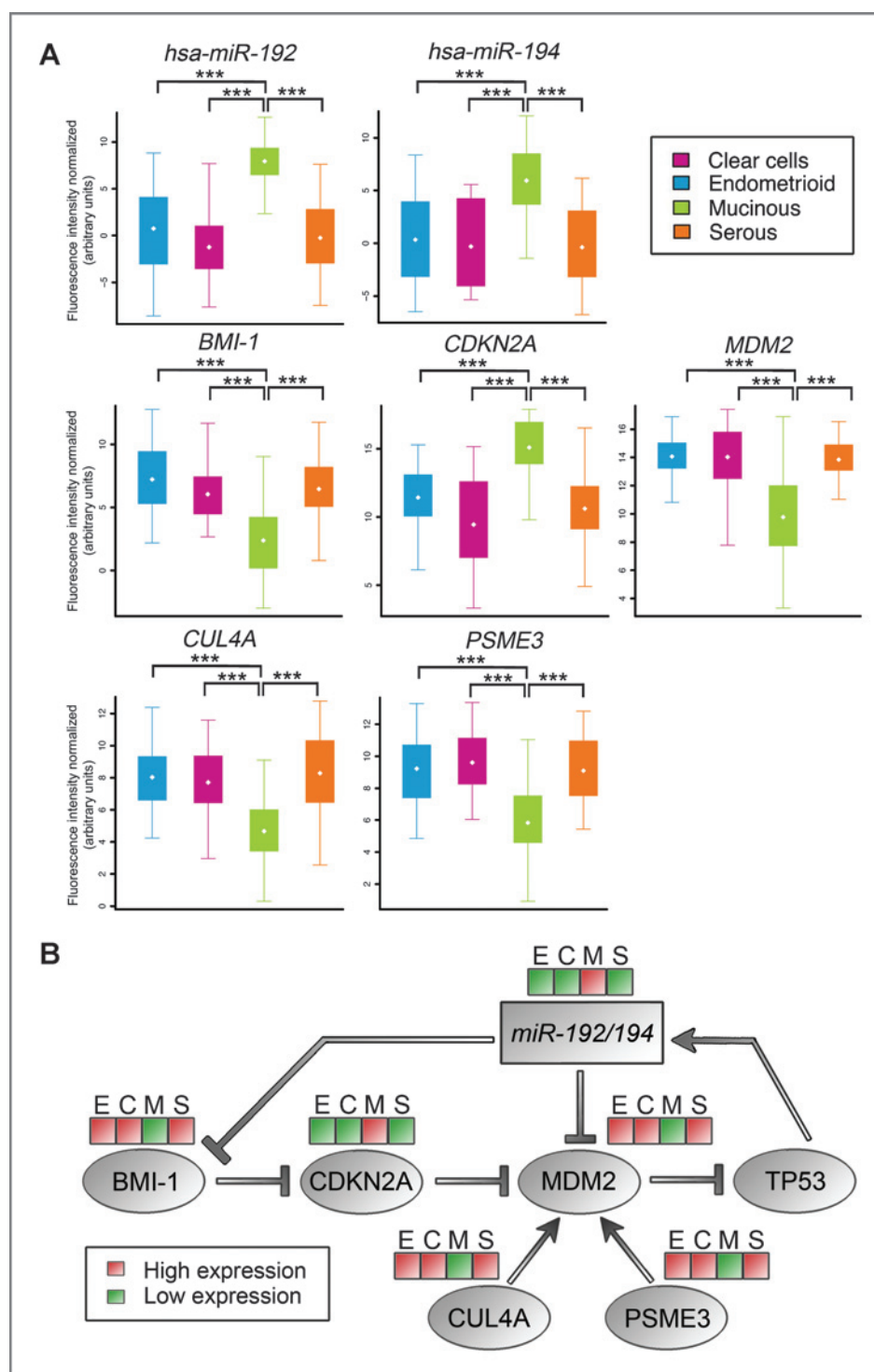
biogenesis, pertinent to DNA metabolism and genome integrity (26). *PTGER3* is a prostanoid receptor, a G-protein–coupled receptor. These genes are involved in multiple genetic diseases, but they have never been associated to EOC. *BMI1*, *PSME3*, and *CUL4A* belong to the p53 regulatory pathway, which differentiates the mucinous from the other ovarian histotypes.

Differential regulation of pathways upstreams p53 in the mucinous EOC

The expression of *miR-192/194* cluster is directly controlled by wild-type *TP53* that, enhancing their transcription, is able to downregulate genes of G_1–G_2 phases, targets of these 2 miRNAs, arresting cell cycle (26). Among the targets of *miR-192/194* is MDM2, a negative

regulator of *TP53* (27). These relationships define a positive feedback loop involving *TP53* that, through *miR-192/194*, inhibits its own inhibitor (Fig. 3B). This positive feedback loop *TP53-miR-192/194-MDM2* confers the status of tumor suppressor to the *miR-192/194* cluster. Recently, the importance of this circuit has been further strengthened by the identification of new oncogenes among the downregulated target genes of these miRNAs (14, 28, 29). In our analysis, *PSME3* and *CUL4A* are promising *miR-192/194* targets, being among the *miR-194* anticorrelated predicted target genes and proteins that physically associate with MDM2 and part of the *TP53* degradation pathway. Specifically, *PSME3* is a proteasome activator that promotes the nuclear export of *TP53* by operating multiple monoubiquitylation, enhancing its physical interaction with MDM2 (30). *CUL4A* is a cullin family member that physically associates with MDM2 and participates as a scaffold in the process of polyubiquitylation of TP53 (31) and in its consequent degradation. However, our binding assay reveals that no direct binding occurs between *miR-194* and any of these 2 genes.

Interestingly, another element linked to this pathway is *BMI1*, a *miR-194* anticorrelated target gene, that is a repressor of the *CDKN2A* protein (32) that prevents the degradation and inactivation of TP53 operated by MDM2 (33). BMI1 belongs to the polycomb group of proteins that form chromatin-modifying complexes commonly deregulated in cancer. *BMI1* is known to be significantly overexpressed in ovarian, endometrial, and cervical cancer compared with normal tissue, and its expression is positively correlated with grade and clinical phases of the disease (34, 35). Notably, *miR-194* binding on *BMI1* mRNA was experimentally validated with the luciferase assay in a panel of endometrial cancer cell lines (14) and reconfirmed by our assay. In our dataset, *BMI1* were negatively correlated with expression levels of *miR-194*, downregulated in mucinous, and upregulated in other histotypes, confirming the differential activation of the signaling circuit in mucinous compared with other EOC subtypes. Finally, *MDM2* expression and *CDKN2A* were evaluated using qRT-PCR in all samples. Mucinous samples showed downregulated *MDM2* expression and upregulated *CDKN2A*, consistently with the expression and the relationship among the other elements of the pathway.

Taken together our results suggest an opposite regulation of TP53 circuit in the mucinous subtype, as compared with the other EOC histotypes.

Conclusions

Ovarian carcinoma histologic subtypes are being recognized as separate disease entities. Nevertheless, current standard treatments are principally guided by the primary origin of organ site and not by commonalities in molecular alterations (36). However, some attempt exists, as an example, the ongoing study led by the Medical Research Council on advanced stage mucinous EOC (Clinical Trial Identifier:

NCT01081262), in which standard paclitaxel–carboplatin chemotherapy is compared with a combination of oxaliplatin/capecitabine, a regimen commonly used in colon cancer.

Given this scenario, the identification of subtype-specific biomarkers and the understanding of mechanisms that characterize the tumor might allow the development of more efficient strategies aimed at improving the diagnosis and treatments.

In summary, our results show that (i) early-stage EOC miRNA pattern is different across subtypes, with no overlaps with miRNA signature generated in normal surface epithelium cells, (ii) mucinous borderline tumors show similar miRNA markers of mucinous tumor of grade 1, 2, and 3, and (iii) early-stage EOC subtypes seem characterized by specific molecular circuits and mechanisms that differentiate the biologic features of different histotypes. In this study, we found that *miR-30a* and *miR-192/194* are key markers, respectively, of clear cell and mucinous subtypes, that are also ideal candidates for developing new therapeutic strategies, as they show the lowest sensitivity to standard carboplatin–paclitaxel chemotherapy (37). Moreover, considering that the miRNA markers are known to play important roles in other cancer diseases, these results hint tantalizingly the possibility to consider our results as the starting point for the study of new EOC treatments. In the light of these findings, we plan to verify our results in sample sets from stage III/IV EOCs, as this could highlight the difference between early and advanced EOCs and potentially clarify for each single histotype the natural progression of the disease.

References

1. Kurman RJ, Shih IeM. The origin and pathogenesis of epithelial ovarian cancer: a proposed unifying theory. Am J Surg Pathol 2010;34:433–43.
2. Prat J. New insights into ovarian cancer pathology. Ann Oncol 2012;23 Suppl 10:x111–7.
3. Köbel M, Kalloger SE, Boyd N, McKinney S, Mehl E, Palmer C, et al. Ovarian carcinoma subtypes are different diseases: implications for biomarker studies. PLoS Med 2008;5:e232.
4. Iorio MV, Visone R, Leva GD, Donati V, Petrocca F, Casalini P, et al. MicroRNA signatures in human ovarian cancer. Cancer Res 2007;67: 8699–707.
5. Ventura A, Jacks T. MicroRNAs and cancer: short RNAs go a long way. Cell 2009;136:586–91.
6. Marchini S, Mariani P, Chiorino G, Marrazzo E, Bonomi R, Fruscio R, et al. Analysis of gene expression in early-stage ovarian cancer. Clin Cancer Res 2008;14:7850–60.
7. Marchini S, Cavalieri D, Fruscio R, Calura E, Garavaglia D, Nerini IF, et al. Association between miR-200c and the survival of patients with stage I epithelial ovarian cancer: a retrospective study of two independent tumour tissue collections. Lancet Oncol 2011;12:273–85.
8. Trimbos JB, Parmar M, Vergote I, Guthrie D, Bolis G, Colombo N, et al. International collaborative ovarian neoplasm trial 1 and adjuvant chemotherapy in ovarian neoplasm trial: two parallel randomized phase III trials of adjuvant chemotherapy in patients with early-stage ovarian carcinoma. J Natl Cancer Inst 2003;95:105–12.
9. Bisognin A, Sales G, Coppe A, Bortoluzzi S, Romualdi C. MAGIA2: from miRNA and genes expression data integrative analysis to microRNA-transcription factor mixed regulatory circuits (2012 update). Nucleic Acids Res 2012;40:W13–21.
10. Sales G, Coppe A, Bisognin A, Biasiolo M, Bortoluzzi S, Romualdi C. MAGIA, a web-based tool for miRNA and Genes Integrated Analysis. Nucleic Acids Res 2010;38:W352–9.
11. Chan JK, Tian C, Monk BJ, Herzog T, Kapp DS, Bell J, et al. Prognostic factors for high-risk early-stage epithelial ovarian cancer: a Gynecologic Oncology Group study. Cancer 2008;112:2202–10.
12. Fruscio R, Corso S, Ceppi L, Garavaglia D, Garbi A, Floriani I, et al. Conservative management of early-stage epithelial ovarian cancer: results of a large retrospective series. Ann Oncol 2013;24:138–44.
13. Gadducci A, Cosio S, Zola P, Sostegni B, Fuso L, Sartori E. Prognostic factors and clinical outcome of patients with recurrent early-stage epithelial ovarian cancer: an Italian multicenter retrospective study. Int J Gynecol Cancer 2013;23:461–8.
14. Dong P, Kaneuchi M, Watari H, Hamada J, Sudo S, Ju J, et al. MicroRNA-194 inhibits epithelial to mesenchymal transition of endometrial cancer cells by targeting oncogene BMI-1. Mol Cancer 2011;10:99.
15. Zhu H, Wu H, Liu X, Li B, Chen Y, Ren X, et al. Regulation of autophagy by a beclin 1-targeted microRNA, miR-30a, in cancer cells. Autophagy 2009;5:816–23.
16. Kreuzaler P, Watson CJ. Killing a cancer: what are the alternatives? Nat Rev Cancer 2012;12:411–24.
17. Reimer D, Hubalek M, Riedle S, Skvortsov S, Erdel M, Concin N, et al. E2F3a is critically involved in epidermal growth factor receptor-directed proliferation in ovarian cancer. Cancer Res 2010;70:4613–23.
18. Reimer D, Hubalek M, Kiefel H, Riedle S, Skvortsov S, Erdel M, et al. Regulation of transcription factor E2F3a and its clinical relevance in ovarian cancer. Oncogene 2011;30:4038–49.
19. Lee H, Park CS, Deftereos G, Morihara J, Stern JE, Hawes SE, et al. MicroRNA expression in ovarian carcinoma and its correlation with clinicopathological features. World J Surg Oncol 2012;10:174.
20. Wyman SK, Parkin RK, Mitchell PS, Fritz BR, O'Briant K, Godwin AK, et al. Repertoire of microRNAs in epithelial ovarian cancer as determined by next generation sequencing of small RNA cDNA libraries. PLoS ONE 2009;4:e5311.
21. Braun CJ, Zhang X, Savelyeva I, Wolff S, Moll UM, Schepeler T, et al. p53-responsive microRNAs 192 and 215 are capable of inducing cell cycle arrest. Cancer Res 2008;68:10094–104.
22. Hino K, Tsuchiya K, Fukao T, Kiga K, Okamoto R, Kanai T, et al. Inducible expression of microRNA-194 is regulated by HNF-1alpha during intestinal epithelial cell differentiation. RNA 2008;14:1433–42.
23. Ma L, Huang Y, Zhu W, Zhou S, Zhou J, Zeng F, et al. An integrated analysis of miRNA and mRNA expressions in non-small cell lung cancers. PLoS ONE 2011;6:e26502.
24. Meng Z, Fu X, Chen X, Zeng S, Tian Y, Jove R, et al. miR-194 is a marker of hepatic epithelial cells and suppresses metastasis of liver cancer cells in mice. Hepatology 2010;52:2148–57.
25. Song B, Wang Y, Kudo K, Gavin EJ, Xi Y, Ju J. miR-192 regulates dihydrofolate reductase and cellular proliferation through the p53-miRNA circuit. Clin Cancer Res 2008;14:8080–6.
26. Stehling O, Vashisht AA, Mascarenhas J, Jonsson ZO, Sharma T, Netz DJA, et al. MMS19 assembles iron-sulfur proteins required for DNA metabolism and genomic integrity. Science 2012;337:195–9.
27. Pichiorri F, Suh S-S, Rocci A, De Luca L, Taccioli C, Santhanam R, et al. Downregulation of p53-inducible microRNAs 192, 194, and 215 impairs the p53/MDM2 autoregulatory loop in multiple myeloma development. Cancer Cell 2010;18:367–81.
28. Feng S, Cong S, Zhang X, Bao X, Wang W, Li H, et al. MicroRNA-192 targeting retinoblastoma 1 inhibits cell proliferation and induces cell apoptosis in lung cancer cells. Nucleic Acids Res 2011;39:6669–78.
29. Yang S, Du J, Wang Z, Yan J, Yuan W, Zhang J, et al. Dual mechanism of deltaEF1 expression regulated by bone morphogenetic protein-6 in breast cancer. Int J Biochem Cell Biol 2009;41:853–61.
30. Liu J, Yu G, Zhao Y, Zhao D, Wang Y, Wang L, et al. REGγ modulates p53 activity by regulating its cellular localization. J Cell Sci 2010;123:4076–84.
31. Nag A, Bagchi S, Raychaudhuri P. Cul4A physically associates with MDM2 and participates in the proteolysis of p53. Cancer Res 2004;64: 8152–5.
32. Kim JH, Yoon SY, Kim C-N, Joo JH, Moon SK, Choe IS, et al. The Bmi-1 oncoprotein is overexpressed in human colorectal cancer and correlates with the reduced p16INK4a/p14ARF proteins. Cancer Lett 2004;203:217–24.
33. Zhang Y, Xiong Y, Yarbrough WG. ARF promotes MDM2 degradation and stabilizes p53: ARF-INK4a locus deletion impairs both the Rb and p53 tumor suppression pathways. Cell 1998;92:725–34.
34. Honig A, Weidler C, Häusler S, Krockenberger M, Buchholz S, Köster F, et al. Overexpression of polycomb protein BMI-1 in human specimens of breast, ovarian, endometrial and cervical cancer. Anticancer Res 2010;30:1559–64.
35. Zhang F, Sui L, Xin T. Correlations of BMI-1 expression and telomerase activity in ovarian cancer tissues. Exp Oncol 2008;30:70–4.
36. Kelemen LE, Köbel M. Mucinous carcinomas of the ovary and colorectum: different organ, same dilemma. Lancet Oncol 2011;12: 1071–80.
37. Alexandre J, Ray-Coquard I, Selle F, Floquet A, Cottu P, Weber B, et al. Mucinous advanced epithelial ovarian carcinoma: clinical presentation and sensitivity to platinum-paclitaxel-based chemotherapy, the GINECO experience. Ann Oncol 2010;21:2377–81.